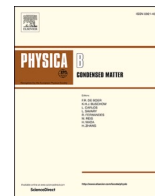




Contents lists available at ScienceDirect

Physica B: Physics of Condensed Matter

journal homepage: <http://www.elsevier.com/locate/physb>

Micromagnetic simulation of domain structure in thin permalloy films with in-plane and perpendicular anisotropy

P.N. Solovev^{a,b,*}, A.V. Izotov^{a,b}, B.A. Belyaev^{a,b}, N.M. Boev^{a,b}

^a Kirensky Institute of Physics, Federal Research Center KSC SB RAS, 50/38 Akademgorodok, 660036, Krasnoyarsk, Russia

^b Siberian Federal University, 79 Svobodny pr., 660041, Krasnoyarsk, Russia

ARTICLE INFO

Keywords:

Micromagnetic simulation
Thin magnetic film
Magnetic anisotropy
Stripe domains
Hysteresis loop
Saturation field

ABSTRACT

We investigate the domain structure formation and magnetization processes in thin permalloy films with in-plane and perpendicular magnetic anisotropy by using micromagnetic simulation. We show that the films of thicknesses less than a critical value L_{cr} are in the monodomain state, and their magnetization processes are specified by the in-plane anisotropy. Above the critical thickness L_{cr} , the perpendicular anisotropy dominates, leading to the formation of the stripe domain structure that significantly complicates the magnetization reversal. The values of the critical thickness, parameters of the domain structure, and the saturation field obtained from the micromagnetic simulations are compared with the corresponding values calculated using analytical expressions derived by Murayama in the framework of the domain structures theory.

1. Introduction

Nanocrystalline soft magnetic thin films, due to their unique properties, find extensive applications in various devices. In particular, such films are used as sensing elements in weak magnetic fields sensors operating on various physical principles—in sensors based on anisotropic magnetoresistance [1], based on a microstrip structure with a thin magnetic film [2–4], in fluxgate sensors [5], and others. The sensitivity of these sensors is usually proportional to the thickness (volume) of a thin film, although the sources of this relationship have different origins for various sensors types [6,7]. Therefore, the search for a way of increasing film's thickness (volume) without deterioration of its magnetic characteristics is an urgent scientific and technological challenge.

Due to the dominant role of the demagnetizing fields, the magnetization of a film in a relatively small external magnetic field lies in its plane. However, when the film thickness exceeds a certain critical value L_{cr} , due to the presence in the film of perpendicular magnetic anisotropy, a periodic stripe domain structure is formed [8]. As experiments show, the transition to the stripe domain state is accompanied by the abrupt change of the film magnetic characteristics, particularly, increase in the coercivity and saturation field, and also the substantial decrease of magnetic permeability [9,10]. Even though in nanocrystalline films the magnetocrystalline anisotropy of individual grains is averaged out due to the exchange interaction [11], other mechanisms exist that can lead

to the formation of perpendicular anisotropy. One of them is associated with the residual mechanical stresses that give contribution to the magnetic energy through the magnetoelastic effect [12]. Another mechanism is related to the formation at specific conditions of the columnar microstructure in the films, with weakened exchange interaction between columns, resulting in the additional magnetostatic contribution to the perpendicular anisotropy [13].

Stripe domain structures in thin magnetic films have been actively studied since the 1960s [8,14]. However, the stripe domains are still the topic of great interest due to their significant role in the formation of various thin film properties, such as magnetotransport [15] or spin wave propagation [16]. Moreover, an analysis of the characteristic behavior of thin films with stripe domains can be used to derive the material parameters of the samples that are hard to obtain by other means [17, 18].

The experimental investigation of magnetic domains is usually limited by the measurements of the magnetization distribution over the film surface, because the determination of the volume distribution is associated with significant technical difficulties [19]. Nevertheless, analytical models can be used for the analysis and interpretation of the experimental data. These models make it possible to theoretically calculate various characteristics of the domain structure depending on the material parameters of the samples [20]. A significant drawback of analytical models is the fact that they initially proceed from a given

* Corresponding author. Kirensky Institute of Physics, Federal Research Center KSC SB RAS, Akademgorodok 50/38, Krasnoyarsk, 660036, Russia.

E-mail address: psolovev@iph.krasn.ru (P.N. Solovev).

<https://doi.org/10.1016/j.physb.2020.412699>

Received 30 September 2020; Received in revised form 3 November 2020; Accepted 7 November 2020

Available online 9 November 2020

0921-4526/© 2020 Elsevier B.V. All rights reserved.

magnetization distribution law, for which the free energy is minimized according to the parameters included in this law. Therefore, using such methods it is impossible to answer the question of whether there are other configurations of magnetization with lower energy.

Thanks to the development of numerical methods for the micromagnetic simulation and a significant increase in the computational power of modern computers, it has recently become possible to investigate complex magnetic structures with high accuracy [21]. In particular, micromagnetic simulation has proven itself as an efficient tool for studying various physical phenomena in thin magnetic films [22–25]. In this paper, using micromagnetic simulation, we study the formation of domain structure and magnetization reversal in thin permalloy films with uniaxial in-plane and perpendicular magnetic anisotropy.

2. Micromagnetic simulation details

The magnetization processes and domain structures formed in thin films were investigated by micromagnetic simulation of a thin film model, in which in-plane and perpendicular magnetic anisotropy were taken into account. The model was discretized on N elements (cubic cells) of volume V_0 . It was assumed that within each cell, the magnetization is uniform and described by a vector $\mathbf{M}^{(i)}$ ($i = 1, 2, \dots, N$), and that the magnetization saturation M_s of the sample is constant. In this case, the free energy F of the film consists of the Zeeman energy, the energy of the exchange and magnetostatic interactions, as well as the energy of the uniaxial in-plane and perpendicular magnetic anisotropy. It can be expressed as [22].

$$F = -V_0 \sum_{i=1}^N \left[HM^{(i)} - \frac{A}{\Delta r^2} \sum_{j=1}^N \left(1 - \frac{M^{(i)} M^{(j)}}{M_s^2} \right) + \frac{1}{2} \sum_{j=1}^N M^{(i)} G_{ij}^{dip} M^{(j)} + \frac{K_u}{M_s^2} (M^{(i)} u)^2 + \frac{K_p}{M_s^2} (M^{(i)} p)^2 \right] \quad (1)$$

where \mathbf{H} is an external magnetic field, A is the exchange constant, Δr is the distance between neighbor cells, G_{ij}^{dip} is a 3×3 tensor that describes the magnetostatic interaction between cells i and j , K_u and K_p are constants of the in-plane and perpendicular uniaxial magnetic anisotropy, and \mathbf{u} and \mathbf{p} are unit vectors coinciding with the directions of the easy axis (EA) for the in-plane and perpendicular anisotropy, respectively. In this study, we have restricted ourselves to the case of a uniform distribution of the magnetic anisotropy parameters in the film. The components of the G_{ij}^{dip} tensor were calculated using an accurate analytical expression obtained in Ref. [26].

To determine the equilibrium magnetization configuration, we used an approach based on the system relaxation according to the internal effective magnetic fields acting on each magnetic moment [22]. On each iteration step, the effective local magnetic field is calculated, and the new distribution of magnetization is set in the direction of the acting force. The iterative process continues until the position of all magnetic moments stabilizes within a given accuracy. It is important to note that the obtained equilibrium magnetization distribution was always checked for stability, and if this test was failed, the new search for the equilibrium distribution in the direction of system relaxation was launched.

We consider the model of a thin film with magnetic parameters corresponding to that of the typical permalloy $\text{Ni}_{80}\text{Fe}_{20}$ film—the saturation magnetization $M_s = 1000 \text{ emu/cm}^3$, the exchange constant $A = 1 \times 10^{-6} \text{ erg/cm}$, the in-plane uniaxial anisotropy field $H_u = 6.5 \text{ Oe}$ ($K_u = H_u M_s / 2 = 3.25 \times 10^3 \text{ erg/cm}^3$), and the perpendicular uniaxial anisotropy field $H_p = 517 \text{ Oe}$ ($K_p = H_p M_s / 2 = 2.58 \times 10^5 \text{ erg/cm}^3$). The in-plane anisotropy EA was oriented along the x -axis, while the perpendicular anisotropy EA lied along the z -axis (normal to the film plane). The size of each discrete element was $6.25 \times 6.25 \times 6.25 \text{ nm}$. We consider the case of the film magnetization by the in-plane external

magnetic field H applied along the hard magnetization axis (HA—the y -axis), or along the EA (the x -axis) of the in-plane anisotropy. Taking into account the symmetry of the problem, the model of the film was discretized on 1024 elements along the x -axis and 64 elements along the y -axis, while along the z -axis the number of elements varied from 8 to 64 depending on the thickness L of the film. Additionally, we used two-dimensional (in the film xy plane) periodic boundary conditions for the exchange and magnetostatic interactions [27]. This allowed us to eliminate the effects from the demagnetizing fields at the film edges [25, 28], thus approximating the characteristics of the simulated films more closely to that of real samples used in practice, for which in-plane sizes are much larger than the thickness.

3. Simulation results and discussion

Using micromagnetic simulation, we investigated the magnetic microstructure (the equilibrium magnetization configuration) and magnetization processes in thin films of various thicknesses $L = 50\text{--}400 \text{ nm}$. It was found that films with thicknesses less than $L_{cr} \approx 125 \text{ nm}$ preserve their uniform monodomain state, and their magnetization curves could be accurately described by the Stoner-Wohlfarth model [29]. The obtained from the hysteresis loops coercivity H_c (when the film was magnetized along the EA) and saturation field H_s (when magnetized along the HA) equaled the in-plane anisotropy field $H_u = 6.5 \text{ Oe}$.

However, of most interest are the films with thicknesses $L > L_{cr}$. As an example, Fig. 1 shows the hysteresis loop obtained for the 200-nm-thick film when the field was applied along the y -axis. Such $M_y(H)$ dependence is characteristic for the films with the magnetic stripe domain structure. The total magnetization component M_y decreases linearly with the decreasing of the field H , starting from the saturation field $H_s = 205 \text{ Oe}$, and then abruptly reverses. As can be seen from the calculated loop, the film has the coercivity $H_c = 128.5 \text{ Oe}$, which is significantly larger than the field of the in-plane magnetic anisotropy.

For the three points on the hysteresis loop (marked on Fig. 1 as “a”, “b”, and “c”), we show in Figs. 2 and 3 the fragments of the equilibrium magnetization distribution. The color in these figures corresponds to the magnetization components M_z (Fig. 2) and M_x (Fig. 3). The arrows display projections of the magnetization vectors on the corresponding planes—two cross-section planes xz and yz , and the film surface (plane xy). Figs. 2a and 3a show magnetic microstructure formed in the 200-nm-thick film in the zero applied field, after the film was magnetized to saturation along the y -axis positive direction. It is clearly seen that the stripe domain structure developed in the film. Periodically alternating regions emerge in the xz plane, in which magnetic moments orient

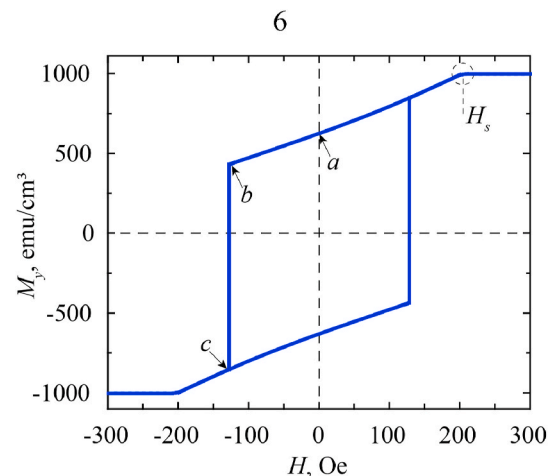


Fig. 1. Magnetization curve of a 200-nm-thick film. The points on the curve marked by the arrows correspond to the distributions shown in Figs. 2 and 3.

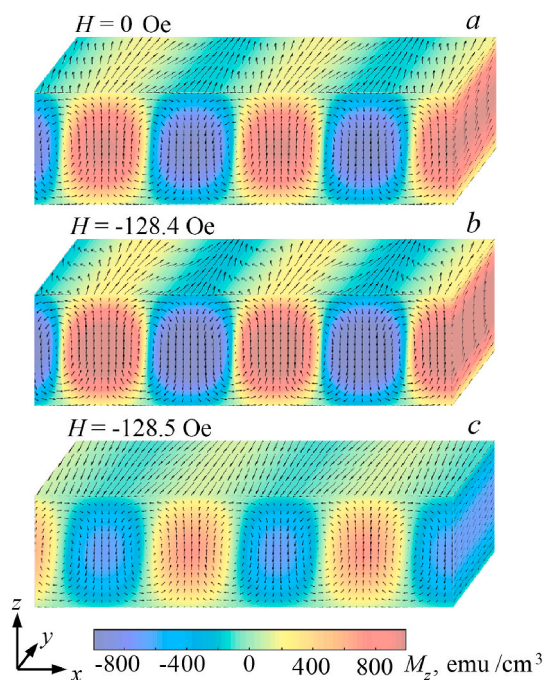


Fig. 2. Distributions of the M_z magnetization component in a 200-nm-thick film, calculated for the three values of the applied field H .

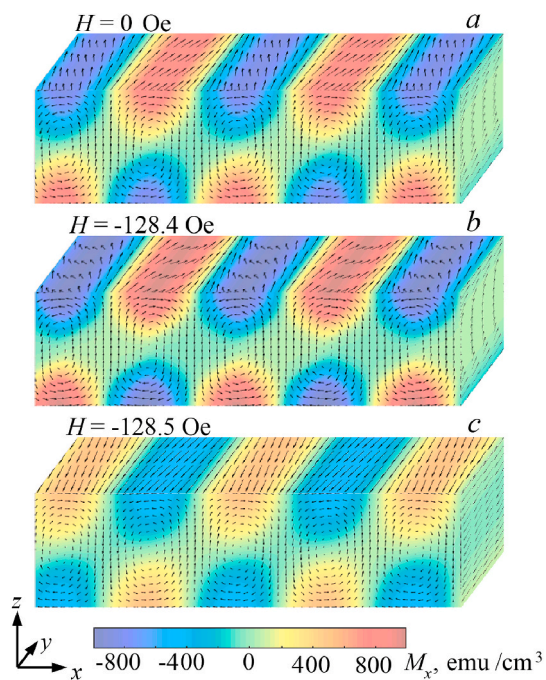


Fig. 3. Distributions of the M_x magnetization component in a 200-nm-thick film, calculated for the three values of the applied field H .

predominantly along the positive or negative direction of the z -axis. Such orientation of the magnetization makes it possible to minimize the contribution to the free energy associated with the perpendicular magnetic anisotropy. In the middle of the film these regions—magnetic domains—are separated by Bloch type domain walls. The magnetization components that are parallel to the film plane gradually increase from the middle to the top and bottom (Fig. 2a). Near the top and bottom film surfaces, closure magnetic domains ensuring closed magnetic flux are formed, as it is best seen in Fig. 3a. Because of that, “magnetic charges”

are almost absent at the film surfaces, resulting in a significantly reduced energy contribution related to the magnetostatic interaction.

An analysis of the magnetic microstructure shows that as the applied field reduces, in the range $-H_c < H < H_s$ the magnetization in the closure domains gradually rotates (the M_y components decrease), while the orientation of the magnetization in the vertical domains near the film center is almost unchanged. This is the process of the reversible magnetization through the rotation. However, this gradual rotation is limited. For the magnetic moments to further orient towards the applied field, the magnetic structure should reconfigure substantially. This is because the change of the magnetization orientation in the closure domains to the opposite direction is inevitably followed by the change in the chirality of the magnetic domain walls, otherwise, the magnetic flux would be open. Therefore, the magnetic moments will orient towards the applied field only when for the current configuration the Zeeman energy will become larger than the energy contributions from the perpendicular anisotropy, and the exchange and magnetostatic interactions. For the considered film this condition is met when $|H| = H_c = 128.5$ Oe. After the applied field reaches this value, the magnetization abruptly reverses in the xy plane in the whole film, while drastically decreased in magnitude M_z component changes its sign in alternating stripes (Figs. 2c and 3c).

From the analysis of the equilibrium magnetization distributions calculated by micromagnetic simulation, it is possible to obtain a number of parameters characterizing the domain structure formed in the films with perpendicular anisotropy. The values of these parameters can be also determined by using analytical expressions derived in the framework of the domain structures theory. These analytical expressions, linking domain parameters with material parameters of the film, give only approximate results. But because of their simplicity and informativity, these expressions are often used while interpreting experimental results. Therefore, it is interesting and practically important to compare results obtained from rigorous micromagnetic computation of the thin film model with the main conclusions of the analytical theory. This will make it possible not only to check the validity of approximations used in the theory but also to determine the limits of its applicability.

In this paper, we investigate the properties of thin permalloy films that, as experimental measurements show, have a relatively small perpendicular magnetic anisotropy. When properties of thin films with perpendicular anisotropy are analyzed, often the parameter $Q = K_p / 2\pi M_s^2$ is considered, known as the quality factor. The quality factor shows the ratio between the perpendicular anisotropy energy and the demagnetizing energy. For the film with the large perpendicular anisotropy, when $Q > 1$, the magnetization direction is parallel (or antiparallel) to the film normal over the entire film. However, for the films having $Q \ll 1$, surface closure domains (with large magnetization components parallel to the film plane) play an important role, supporting the state with lower free energy [20]. For the parameters of the film used in the simulations, the value of Q is 0.04.

In the paper published in 1966 [30], Yoshimasa Murayama introduced a theoretical model of a thin film with moderate perpendicular anisotropy, restricting to the case of $Q < 1$. Unlike the earlier model of the domain structure [8], the Murayama model takes into account not only the out-of-plane rotation of magnetization but also the in-plane rotation, thus providing the possibility of closure domains formation. From the approximate solution of the developed model, Murayama derived analytical equations allowing for the determination of domain structure’s main characteristics.

One of the most important characteristics of thin films with perpendicular anisotropy is the critical thickness L_{cr} . It determines the boundary of the second-order magnetic phase transition from the in-plane uniform magnetization to the out-of-plane noncollinear magnetic structure (stripe domains). Murayama obtained the following well-known formula for the L_{cr}

$$L_{cr} = 2\pi\sqrt{A/K_p} \quad (2)$$

It should be noted that the expression (2) does not include saturation magnetization M_s . As the Murayama model considers surface closure domains, the demagnetizing energy does not contribute to L_{cr} . Fig. 4 shows the dependence of the critical thickness on the perpendicular anisotropy field. The line corresponds to the calculation using expression (2), while symbols are the results of the micromagnetic simulation. One can see a good agreement between the simulation and the theory of Murayama.

The micromagnetic simulation results show that in the films with thicknesses equal or slightly larger than L_{cr} , a periodic magnetic microstructure is formed, without clearly defined domain boundaries. Such distribution of magnetization is usually called the weak-stripe domain structure [20]. As an example, in Fig. 5a, we show the equilibrium magnetization configuration calculated for the film of thickness $L = 125$ nm. In the xz plane, the alternating vortex-like structures emerge, representing a transition phase to the stripe domains. For such films, it is difficult to define unambiguously the width of the stripe domain. In this regard, we have introduced the following two characteristics. The first, D , equals the half-period of the M_z component distribution in the film center along the x -axis (see Fig. 5b). This definition of the domain width is often used in analytical models. The second characteristic, D' , is defined as the width (along the x -axis) of a region in the film center, in which the M_z component is at least 65% of its maximum magnitude. We note that the value of 65% is somewhat arbitrary, and it was chosen because in this limit in the middle of the 125-nm-thick film, magnetic moments deviate from their average orientation on no more than $\sim 3.5^\circ$ in the xz -plane. Therefore, D corresponds to the width of the domain and domain wall taken together, while D' approximately equals the width of the domain itself.

It is interesting to compare the values of parameters D and D' , obtained from the numerical simulation of the films of various thicknesses, with the stripe domain width calculated according to the analytical expression derived by Murayama

$$D_M = \sqrt{L^4 \sqrt{\pi A (K_p + 2\pi M_s^2)} / 2K_p M_s^2} \quad (3)$$

Fig. 5c demonstrates the dependencies of the stripe domain width on the film thickness. The symbols show the parameters D and D' , while the solid line corresponds to the results obtained according to expression (3). Additionally, the dashed line on the figure shows the domain width versus film thickness calculated according to the equation $D_K = 2.82\sqrt{L^4 \sqrt{A/K_p}}$ obtained by Kittel while considering Landau domain structures [31]. For the thicknesses slightly larger than L_{cr} , there is a

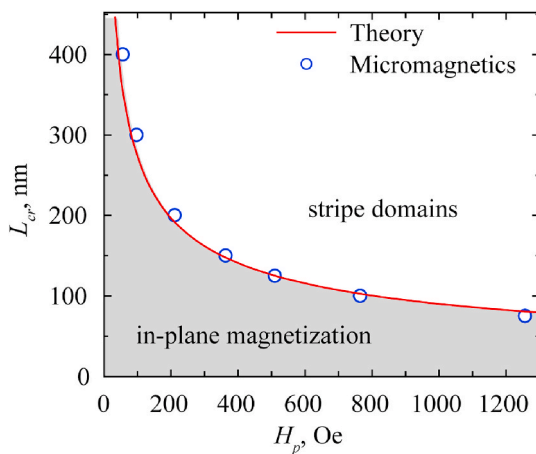


Fig. 4. The critical thickness L_{cr} versus the perpendicular anisotropy field H_p . The line is the theoretical calculation (the Murayama model), and the symbols are the micromagnetic simulation.

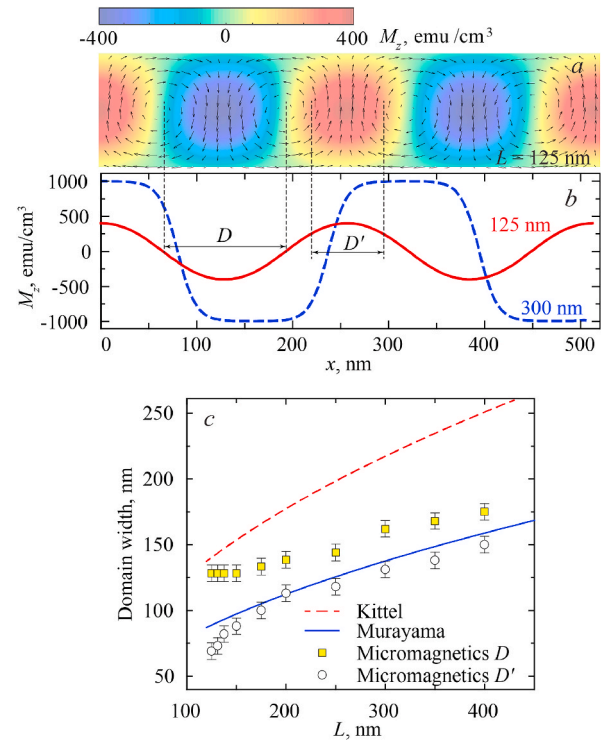


Fig. 5. (a) Magnetization distribution in the xz plane of the film with thickness 125 nm; (b) M_z component distribution along the x -axis in the center of films with thicknesses of 125 and 300 nm; (c) stripe domain width versus film thickness. The symbols are the parameters obtained from the micromagnetic simulation, the solid line is the Murayama model, and the dashed line is the Kittel model.

marked discrepancy between the results of micromagnetic simulation and the calculation according to expression (3). Noteworthy is the behavior of the parameters D and D' . With the increase of the film thickness from L_{cr} to 150 nm, D remains almost constant, while D' increases. This indicates that in this range of thicknesses, the domain wall width begins to reduce. However, after L reaches 150 nm, both values start to grow, approaching from the above and below to the results of the theory of Murayama. At the same time, the domain width calculated using Kittel's expression turns out to be significantly overestimated. In both models, Murayama and Kittel, the domain width is proportional to the square root of the film thickness, but with different coefficients. In the Murayama model, this coefficient is smaller because it includes magnetization saturation. In other words, in this model, it is considered that the magnetic flux is not fully closed, as it was assumed in the Kittel model but there is some energy associated with the demagnetizing fields. This energy can be neglected when calculating the critical thickness but not the domain width, which is in good accordance with the micromagnetic simulation. Thus, these results show that for the analysis of the films with $Q \ll 1$, it is preferable to use the Murayama model.

The discrepancy between the results of the theory of Murayama and micromagnetic simulation for the domain width in the case of $L \sim L_{cr}$ is due to the formation of the weak-stripe domain structure, that was not considered in the Murayama model. However, with the thickness increasing, magnetic domains with well-defined boundaries begin to emerge. This is seen in Fig. 6, where magnetization distributions in the cross-section xz plane calculated for various thicknesses are shown. The color here corresponds to the projection of the magnetization vector on the x -axis reduced to its maximum value for the film of thickness L , $M_x/M_x^{max}(L)$. As the thickness increases, well-defined vertical domains appear. The closure domains result in formation on the film surface stripe periodic structures, which are observed in experiments. We also

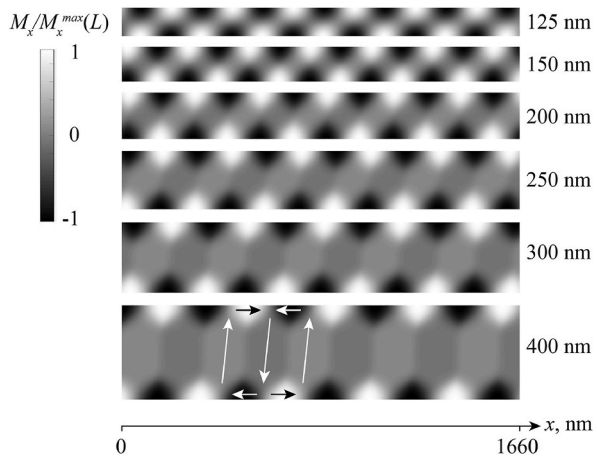


Fig. 6. Distribution of the magnetization vector projection on the x -axis (M_x component) in the xz plane of the films of various thicknesses. Here white color corresponds to the positions of the reduced M_x maximums, and black to the minimums.

note that the domain wall is slightly inclined ($\sim 5^\circ$) with respect to the film normal, which is especially noticeable for the “thick” films. Apparently, this inclination is caused by the in-plane uniaxial anisotropy, which EA lies along the x -axis.

Another important characteristic is the saturation field H_s . In an ideal film of thickness $L < L_{cr}$, which is in a state of uniform magnetization, H_s is determined by the in-plane uniaxial anisotropy field. However, for the films with stripe domains, the saturation field has a more complex dependency on the film parameters. Murayama derived the following equation for H_s

$$1 - \frac{H_s}{H_p} = \frac{L_{cr}}{L} \left[1 + \frac{K_p}{2\pi M_s^2} \right]^{-1/2} \quad (4)$$

Fig. 7 shows the dependencies of the saturation field H_s on the film thickness calculated according to expression (4) (solid line) and obtained from the magnetization curves calculated by micromagnetic simulation. For the films with $L > L_{cr}$, there is a very good agreement between the theory and simulation. This demonstrates that expression (4) can be used in a simple technique of determining perpendicular anisotropy constant K_p from the measured in-plane saturation field.

Indeed, expression (4) can be rewritten as a cubic equation for the K_p in the form

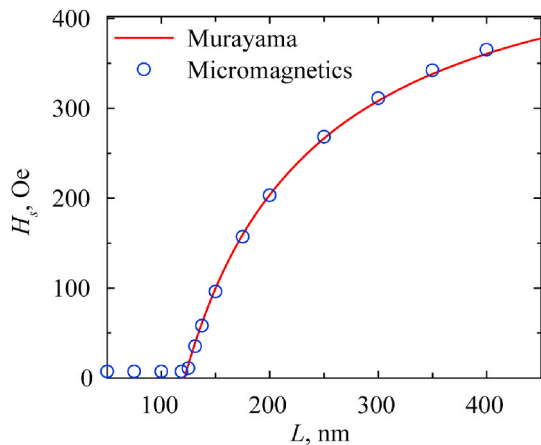


Fig. 7. The saturation field H_s versus the film thickness L . The line is the calculation according to the Murayama theory, the symbols are the micromagnetic simulation results.

$$aK_p^3 + bK_p^2 + cK_p + d = 0,$$

$$a = 4L^2, b = 4L^2 M_s (2\pi M_s - H_s),$$

$$c = M_s^2 (L^2 H_s^2 - 8\pi L^2 H_s M_s + 32\pi^3 A),$$

$$d = 2\pi L^2 H_s^2 M_s^4. \quad (5)$$

Thus, if we know the thickness L , the saturation magnetization M_s and the exchange constant A of the film, we can calculate K_p using the experimental value of the saturation field H_s obtained from an in-plane hysteresis loop. It should be noted that equation (5) has three roots, but its numerical calculation for the parameters of the considered film showed that one of the roots was negative, while the value of a second one was an order of magnitude less than the initial K_p . Putting the H_s values found using micromagnetic simulation for films of different thicknesses into Eq. (5), we plotted in Fig. 8 dependence of $H_p = 2K_p/M_s$ on thickness L . The dashed line on the figure shows the value of H_p used in the simulation. One can see that calculated from the hysteresis loops value of H_p is close to the initial value, with the maximum relative error of about 4.5%.

4. Conclusion

In this paper, using micromagnetic simulation, we investigated domain structure and magnetization processes of thin permalloy films with the in-plane and perpendicular magnetic anisotropy. For the film thicknesses L less than the critical value L_{cr} , the in-plane anisotropy plays a decisive role in the magnetization processes, and the static properties of such films are accurately described by the Stoner-Wohlfarth model. In films with $L > L_{cr}$, the influence of the perpendicular anisotropy becomes dominant resulting in the formation of the stripe domain structure and, as a consequence, in sharp increase of the saturation field and coercivity. An analysis of the magnetic microstructure and magnetization processes of the films in the stripe domain phase demonstrated a general good agreement between the results of the micromagnetic simulation and the theoretical model introduced by Murayama [30]. However, a discrepancy between the simulation and the Murayama model was found for the domain width in the films with $L \sim L_{cr}$. It was shown that this discrepancy is associated with the development in the films of such thicknesses of the weak-stripe domain structure, that was not taken into account in the Murayama model. We showed that by using an analytical expression derived by Murayama for the saturation field, it is possible to determine the perpendicular anisotropy constant from the in-plane measured hysteresis loop. The presented study might be of particular interest for developers of a number of practical devices based on soft magnetic thin films.

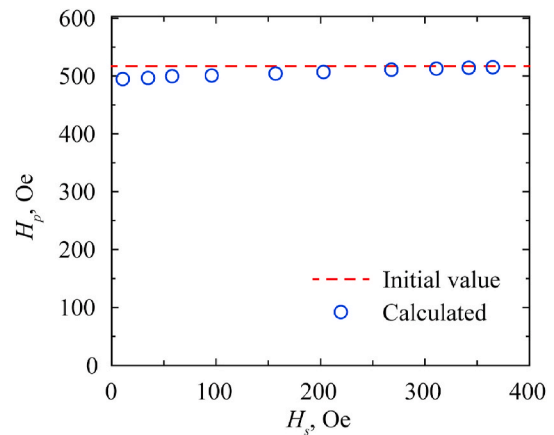


Fig. 8. The values of the perpendicular anisotropy field H_p , obtained from the hysteresis loops using Eq. (5) (symbols). The dashed line shows the initial value of H_p .

CRedit authorship contribution statement

P.N. Solovev: Conceptualization, Methodology, Software, Writing - original draft, Writing - review & editing, Supervision. **A.V. Izotov:** Conceptualization, Writing - original draft, Writing - review & editing, Visualization. **B.A. Belyaev:** Conceptualization, Supervision, Writing - review & editing, Funding acquisition. **N.M. Boev:** Methodology, Software, Writing - review & editing.

Declaration of competing interest

The authors declare that they have no known competing financial interests or personal relationships that could have appeared to influence the work reported in this paper.

Acknowledgement

This work was supported by the Ministry of Science and Higher Education of the Russian Federation, agreement number 075-11-2019-054 dated 22.11.2019.

References

- [1] C. Wang, W. Su, Z. Hu, J. Pu, M. Guan, B. Peng, L. Li, W. Ren, Z. Zhou, Z. Jiang, M. Liu, Highly sensitive magnetic sensor based on anisotropic magnetoresistance effect, *IEEE Trans. Magn.* 54 (2018) 1–3, <https://doi.org/10.1109/TMAG.2018.2846758>.
- [2] H. Uetake, T. Kawakami, S. Yabukami, T. Ozawa, N. Kobayashi, K.I. Arai, Highly sensitive coplanar line thin-film sensor using SrTiO film, *IEEE Trans. Magn.* 50 (2014) 1–4, <https://doi.org/10.1109/TMAG.2014.2331676>.
- [3] A.N. Babitskii, B.A. Belyaev, N.M. Boev, G.V. Skomorokhov, A.V. Izotov, R. G. Galeev, A magnetometer of weak quasi-stationary and high-frequency fields on resonator microstrip transducers with thin magnetic fields, *Instrum. Exp. Tech.* 59 (2016) 425–432, <https://doi.org/10.1134/S0020441216030131>.
- [4] A.N. Babitskii, B.A. Belyaev, N.M. Boev, A.V. Izotov, Low noise wideband thin-film magnetometer, in: *IEEE SENSORS, IEEE*, 2017, pp. 316–318, <https://doi.org/10.1109/ICSENS.2017.8233972>. Glasgow, 2017.
- [5] S.M. Choi, T. Lee, C.-S. Yang, K.-H. Shin, S.H. Lim, Effects of lateral dimensions of the magnetic thin films on the characteristics of thin-film type orthogonal fluxgate sensors, *Thin Solid Films* 565 (2014) 271–276, <https://doi.org/10.1016/j.tsf.2014.06.026>.
- [6] C. Tannous, J. Gieraltowski, Giant magneto-impedance and its application, *J. Mater. Sci. Mater. Electron.* 15 (2004) 125–133, <https://doi.org/10.1023/B:JMSE.0000011350.93694.91>.
- [7] N. Smith, P. Arnett, Thermal magnetization noise in spin valves, *IEEE Trans. Magn.* 38 (2002) 32–37, <https://doi.org/10.1109/TMAG.2002.988907>.
- [8] N. Saito, H. Fujiwara, Y. Sugita, A new type of magnetic domain structure in negative magnetostriction Ni-Fe films, *J. Phys. Soc. Jpn.* 19 (1964) 1116–1125, <https://doi.org/10.1143/JPSJ.19.1116>.
- [9] J. Wei, Z. Zhu, H. Feng, J. Du, Q. Liu, J. Wang, Top-down control of dynamic anisotropy in permalloy thin films with stripe domains, *J. Phys. Appl. Phys.* 48 (2015) 465001, <https://doi.org/10.1088/0022-3727/48/46/465001>.
- [10] D. Cao, L. Pan, X. Cheng, Z. Wang, H. Feng, Z. Zhu, J. Xu, Q. Li, S. Li, J. Wang, Q. Liu, Thickness-dependent on the static magnetic properties and dynamic anisotropy of FeNi films with stripe domain structures, *J. Phys. Appl. Phys.* 51 (2018), 025001, <https://doi.org/10.1088/1361-6463/aa9c31>.
- [11] G. Herzer, Modern soft magnets: amorphous and nanocrystalline materials, *Acta Mater.* 61 (2013) 718–734, <https://doi.org/10.1016/j.actamat.2012.10.040>.
- [12] B.A. Belyaev, A.V. Izotov, Ferromagnetic resonance study of the effect of elastic stresses on the anisotropy of magnetic films, *Phys. Solid State* 49 (2007) 1731–1739, <https://doi.org/10.1134/S106378340709020X>.
- [13] P.N. Solovev, A.V. Izotov, B.A. Belyaev, Microstructural and magnetic properties of thin obliquely deposited films: a simulation approach, *J. Magn. Magn. Mater.* 429 (2017) 45–51, <https://doi.org/10.1016/j.jmmm.2017.01.012>.
- [14] Y. Sugita, H. Fujiwara, T. Sato, Critical thickness and perpendicular anisotropy of evaporated permalloy films with stripe domains, *Appl. Phys. Lett.* 10 (1967) 229–231, <https://doi.org/10.1063/1.1754924>.
- [15] B. Pianciola, S. Flewett, E. De Biasi, C. Hepburn, L. Lounis, M. Vázquez-Mansilla, M. Granada, M. Barturen, M. Eddrief, M. Sacchi, M. Marangolo, J. Milano, Magnetoresistance in Fe_{0.8}Ga_{0.2} thin films with magnetic stripes: the role of the three-dimensional magnetic structure, *Phys. Rev. B* 102 (2020), 054438, <https://doi.org/10.1103/PhysRevB.102.054438>.
- [16] C. Liu, S. Wu, J. Zhang, J. Chen, J. Ding, J. Ma, Y. Zhang, Y. Sun, S. Tu, H. Wang, P. Liu, C. Li, Y. Jiang, P. Gao, D. Yu, J. Xiao, R. Duine, M. Wu, C.-W. Nan, J. Zhang, H. Yu, Current-controlled propagation of spin waves in antiparallel, coupled domains, *Nat. Nanotechnol.* 14 (2019) 691–697, <https://doi.org/10.1038/s41565-019-0429-7>.
- [17] K.-W. Moon, J. Yoon, J.W. Choi, C. Kim, D.-O. Kim, D. Kim, B.S. Chun, B.-C. Min, C. Hwang, Measuring the magnetization from the image of the stripe magnetic domain, *Phys. Rev. Applied.* 12 (2019), 034030, <https://doi.org/10.1103/PhysRevApplied.12.034030>.
- [18] J. McCord, B. Erkartal, T. von Hofe, L. Kienle, E. Quandt, O. Roshchupkina, J. Grenzer, Revisiting magnetic stripe domains — anisotropy gradient and stripe asymmetry, *J. Appl. Phys.* 113 (2013), 073903, <https://doi.org/10.1063/1.4792517>.
- [19] J.N. Chapman, R.P. Ferrier, Strong stripe domains: II. investigations into the two-dimensional nature of domain walls, *Phil. Mag.: A Journal of Theoretical Experimental and Applied Physics* 28 (1973) 581–595, <https://doi.org/10.1080/14786437308221004>.
- [20] A. Hubert, R. Schäfer, *Magnetic Domains*, Springer, Berlin, 1998.
- [21] L. Lopez-Diaz, D. Aurelio, L. Torres, E. Martinez, M.A. Hernandez-Lopez, J. Gomez, O. Alejos, M. Carpentieri, G. Finocchio, G. Consolo, Micromagnetic simulations using graphics processing units, *J. Phys. Appl. Phys.* 45 (2012) 323001, <https://doi.org/10.1088/0022-3727/45/32/323001>.
- [22] B.A. Belyaev, A.V. Izotov, An.A. Leksikov, Micromagnetic calculation of the equilibrium distribution of magnetic moments in thin films, *Phys. Solid State* 52 (2010) 1664–1672, <https://doi.org/10.1134/S1063783410080160>.
- [23] B.A. Belyaev, A.V. Izotov, Micromagnetic calculation of magnetostatic oscillation modes of an orthogonally magnetized disk of yttrium iron garnet, *Phys. Solid State* 55 (2013) 2491–2500, <https://doi.org/10.1134/S1063783413120068>.
- [24] A.V. Izotov, B.A. Belyaev, P.N. Solovev, N.M. Boev, Numerical calculation of high frequency magnetic susceptibility in thin nanocrystalline magnetic films, *Phys. B Condens. Matter* 556 (2019) 42–47, <https://doi.org/10.1016/j.physb.2018.12.006>.
- [25] B.A. Belyaev, A.V. Izotov, G.V. Skomorokhov, P.N. Solovev, Micromagnetic analysis of edge effects in a thin magnetic film during local excitation of magnetization oscillations, *Russ. Phys. J.* (2020), <https://doi.org/10.1007/s11182-020-02106-3>.
- [26] A.J. Newell, W. Williams, D.J. Dunlop, A generalization of the demagnetizing tensor for nonuniform magnetization, *J. Geophys. Res.* 98 (1993) 9551, <https://doi.org/10.1029/93JB00694>.
- [27] K.M. Lebecki, M.J. Donahue, M.W. Gutowski, Periodic boundary conditions for demagnetization interactions in micromagnetic simulations, *J. Phys. Appl. Phys.* 41 (2008) 175005, <https://doi.org/10.1088/0022-3727/41/17/175005>.
- [28] B.A. Belyaev, A.V. Izotov, G.V. Skomorokhov, P.N. Solovev, Experimental study of the magnetic characteristics of nanocrystalline thin films: the role of edge effects, *Mater. Res. Express* 6 (2019) 116105, <https://doi.org/10.1088/2053-1591/ab4456>.
- [29] E.C. Stoner, E.P. Wohlfarth, A mechanism of magnetic hysteresis in heterogeneous alloys, *Phil. Trans. Roy. Soc. Lond. Math. Phys. Sci.* 240 (1948) 599–642, <https://doi.org/10.1098/rsta.1948.0007>.
- [30] Y. Murayama, Micromagnetics on stripe domain films. I. Critical cases, *J. Phys. Soc. Jpn.* 21 (1966) 2253–2266, <https://doi.org/10.1143/JPSJ.21.2253>.
- [31] C. Kittel, Theory of the structure of ferromagnetic domains in films and small particles, *Phys. Rev.* 70 (1946) 965–971, <https://doi.org/10.1103/PhysRev.70.965>.